remote sensing

MDPI

A Methodology to Monitor Urban Expansion and Green Space Change Using a Time Series of Multi-Sensor SPOT and Sentinel-2A Images

Jinsong Deng [1], Yibo Huang [1], Binjie Chen [1], Cheng Tong [1], Pengbo Liu [1], Hongquan Wang [1],* and Yang Hong [2]

[1] College of Environmental and Resource Sciences, Zhejiang University, Hangzhou 310058, China; jsong_deng@zju.edu.cn (J.D.); yiboh@zju.edu.cn (Y.H.); 3130103023@zju.edu.cn (B.C.); 21714124@zju.edu.cn (C.T.); 3160102573@zju.edu.cn (P.L.)

[2] School of Civil Engineering and Environmental Sciences, University of Oklahoma, Norman, OK 73019, USA; hongyang@ou.edu

* Correspondence: hongquan_wang@zju.edu.cn

check for updates

Abstract: Monitoring urban expansion and greenspace change is an urgent need for planning and decision-making. This paper presents a methodology integrating Principal Component Analysis (PCA) and hybrid classifier to undertake this kind of work using a sequence of multi-sensor SPOT images (SPOT-2,3,5) and Sentinel-2A data from 1996 to 2016 in Hangzhou City, which is the central metropolis of the Yangtze River Delta in China. In this study, orthorectification was first applied on the SPOT and Sentinel-2A images to guarantee precise geometric correction which outperformed the conventional polynomial transformation method. After pre-processing, PCA and hybrid classifier were used together to enhance and extract change information. Accuracy assessment combining stratified random and user-defined plots sampling strategies was performed with 930 reference points. The results indicate reasonable high accuracies for four periods. It was further revealed that the proposed method yielded higher accuracy than that of the traditional post-classification comparison approach. On the whole, the developed methodology provides the effectiveness of monitoring urban expansion and green space change in this study, despite the existence of obvious confusions that resulted from compound factors.

1. Introduction

Rapid urbanization and exploitation of natural resources have raised increasing concerns over environmental issues and made the urban area into a fragile region. It is especially true in the coastal developed urban area in China [1–5]. A wide variety of green spaces of different sizes could help solve many urban diseases and improve the quality of life for urban residents, as urban green spaces provide a wide range of ecosystem services [6–8]. Green space is an essential element in maintaining the urban ecological environment and human well-being, but areas with rapid green space loss might suggest high vulnerability to urban expansion [9]. The green spaces usually include community parks, woodlands, nature reserves and agricultural lands [10]. With the population increase and expansion of cities, more and more open space, woodland and cultivated land have been converted into construction land due to the increasing demands for transportation land, commercial land and residential land. At the same time, the demand for various types of agricultural products has also led to the conversion of some forest land and agricultural land into flower bases or agricultural bases [11]. Therefore, monitoring urban expansion and green space change has been the primary task for urban management

and been elevated to the forefront of research and practical applications [12,13]. The utilization of remote sensing technology with high-frequency and high-resolution has made it possible to precisely trace the intensity of land use on a large scale and in a cost-effective way [14]. Actually, a large number of urban remote sensing investigations since the launch of the first SPOT satellite in 1986 have implied that the tool is already operational and perhaps worthy of widespread development and application [15–17].

The urban environment typically represents a substantial heterogeneity and mixture of land use/cover types. Thus, successfully monitoring urban expansion and green space change requires an adequate understanding of landscape features, selection of suitable data and appropriate change detection method adopted in relation to the aims of application. Moreover, remote sensing data used for urban applications must meet specific conditions in terms of temporal, spatial, spectral and radiometric characteristics [18–20]. Among these issues, the technical concern, over the years in urban applications, has been the pursuit of finer spatial resolutions of images [21–23]. The commonly used Landsat data with 30 m resolution is not able to capture most of the small land cover patterns and land use changes [24]. Thus, the remote sensing data with the spatial resolution corresponding to 0.5–10 m Instantaneous Field of View are required to adequately define the high-frequency detail which characterizes the urban scenes [25]. However, the implementations of conventional methods of data-related modeling were usually hampered by several limitations, such as the availability of archive data, data quality and data distributors. Therefore, it is difficult to conduct long-term monitoring of urban land-use change by using historical high spatial resolution satellite data, especially in China. In recent decades, satellite imagery with similar spatial-resolution to SPOT satellites have become increasingly available. Many pieces of research indicate that the satellites such as ZY1-02C, ZY3, GF-1 and GF-2 launched by China have provided sufficient data sources for monitoring urban expansion and green space change effectively [26–30]. Additionally, the European Space Agency launched the Sentinel sensors, making it easier to obtain high-resolution satellite images [31]. Thus, many scholars use recent images provided by Sentinel satellites to monitor green space changes and urban expansion [32–36]. The use of SPOT imagery and these recently available data enables us to monitor urban expansion and green space change over long periods.

Moreover, the appropriate selection of change detection methods is as crucial to urban monitoring application as the choice of remote sensing data. Generally, change detection can be summarized into broad categories, either post-classification comparison or pre-classification spectral change detection methods. General description and comparison of the underlying advantage or disadvantage in these two broad categories are given in the literature [23,37–42]. Although many factors could affect the selection of land change detection methods, post-classification, Principal Component Analysis (PCA) and image differencing are often used in practice, and they can perform better than other methods. [23,43–46]. However, one major challenge confronting the remote sensing change detection is to identify a method that practically matches particular applications. Generally speaking, when selecting remote sensing data for change detection applications, it is essential to use the data with the same sensor characteristics and anniversary or very near anniversary acquisition dates in order to eliminate the effects of external sources such as sun angle and seasonal and phenological differences [23]. However, in most cases, the remote sensing data comes from different sensors, and they are inter-operated in these sensors. It is difficult to obtain sequential data from a single sensor with similar acquisition dates. Therefore, a suitable change detection method can, not only process the multi-sensor data with differing acquisition dates and spectral modes, but also provide accurate information of change with as little pre-processing as possible while handling cost and time.

For the aforementioned importance and reasons, the central objective of this paper is to present a practical and cost-effective land use change detection method that integrates a multi-date PCA and hybrid classifier by adopting a time series of multi-sensor SPOT and Sentinel-2A images spanning the past 20 years (1996–2016) in order to provide critical and reliable information for the Hangzhou City planning agency. The detection method provided by this study can not only provide solutions for

monitoring land use and urban expansion in the future but also can be used in other cities to achieve moderate urban expansion and coordinated development of the social economy.

2. Materials and Methods

2.1. Study Area

The study area lies in Hangzhou City, the capital of Zhejiang province and the central metropolis of the south wing of the Yangtze River Delta (Figure 1). Hangzhou City covers an area of 3.068 km^2 (720 km^2 for City Proper) with a population of 3.93 million. It has been renowned internationally for its scenic attractions and also as one of the centers of Chinese history and culture spanning back over 2000 years. Hangzhou City is among the top five most economically competitive cities in mainland China and was awarded the Best Chinese Destination for Investment. Hangzhou City now has 166.5 km^2 of green space construction, and green space covers about 40% of urban space [8,47]. Concomitant with stepped-up economic development and industrialization, and tremendous immigration, Hangzhou City is facing the challenges of rapid urbanization and land change.
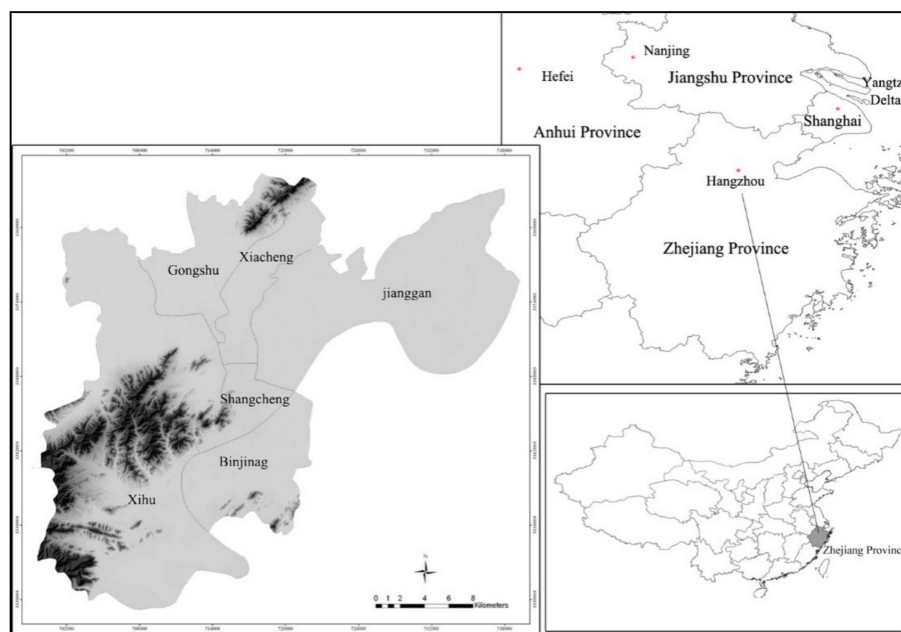

Figure 1. Location of Hangzhou City in Yangtze River Delta.

2.2. Data Source

Owing to the data-related limitations, altogether five scenes of cloud-free SPOT images and one Sentinel-2A image during the 20-year span (1996–2016) are available for the study area. The multi-temporal data series comprises of three SPOT sensors (SPOT-2, SPOT-3 and SPOT-5), Sentinel sensor (Sentinel-2A) and two spectral modes (XS and PAN). Table 1 documents the characteristics of the selected data. The main reference and ancillary data used in this study are land use map (1996), aerial photograph (2000), IKONOS image (2003), QUICKBIRD image (2006), GF-2 and WorldView images (2016 and 2017). In addition, the field surveys were carried out in 2003 and 2006 respectively including GPS positioning, taking photos and inquiring of farmers about the land use history. Land use data interpreted from high-resolution image and on-site surveys in 2016 were also collected.

Table 1. Sensor system characteristics of remote sensing data used in this study.

Acquisition Date	Sensor	Instrument	Spectral Mode	Spectral Resolution (µm)	Spatial Resolution (m)
25-03-2016	Sentinel-2A	MSI	XS	0.46–0.52 0.54–0.58 0.65–0.68 0.79–0.90	10
21-12-2006	SPOT-5	HRG	XS	0.50–0.90 0.61–0.68 0.78–0.89	10
				1.58–1.75	20
06-03-2003	SPOT-5	HRG	XS	0.50–0.90 0.61–0.68 0.78–0.89	10
				1.58–1.75	20
29-03-2000	SPOT-2	HRV	XS	0.50–0.90 0.61–0.68 0.78–0.89	20
22-04-1996	SPOT-3	HRV	PAN	0.51–0.73	10

Note: MSI—Multi Spectral Instrument; HRV—High Resolution Visible; HRG—High Resolution Geometric Imaging Instrument; XS—Multispectral Mode; PAN—Panchromatic Mode.

2.3. Methods

2.3.1. Flowchart

The main procedure of the proposed methodology is diagrammatized in Figure 2 and a detailed depiction is given in the following four sub-sections.
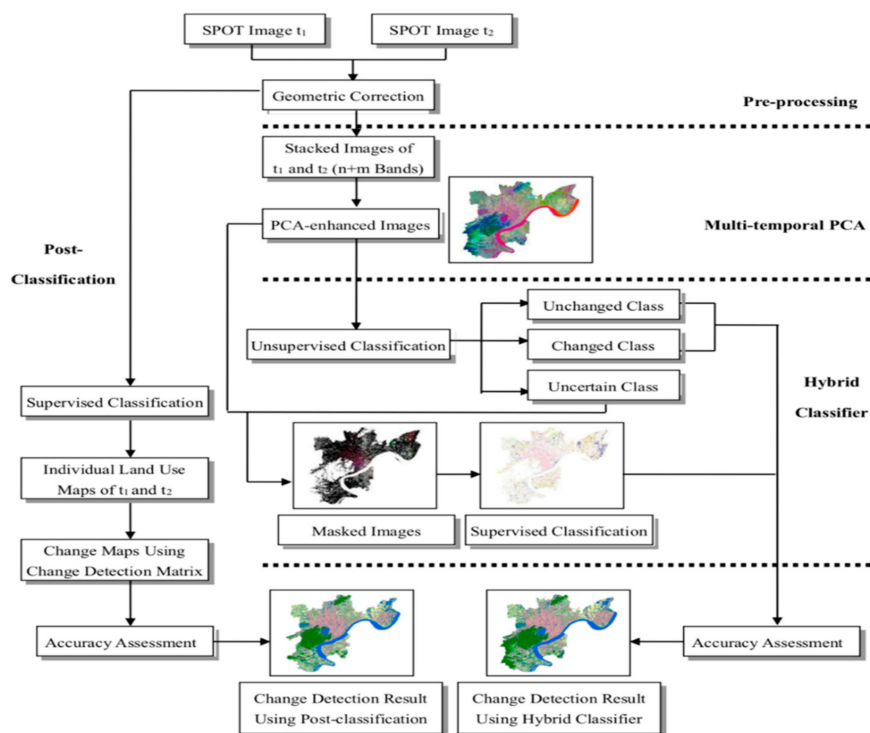

Figure 2. The flowchart of the proposed methodology and post-classification comparison change detection.

2.3.2. Pre-Processing

Geometric corrections including image-to-image rectification and image-to-image registration are the most important pre-processing steps for multi-temporal change detection. It has been strongly suggested that the root mean square (RMS) error between any two dates does not exceed 0.5 pixels to eliminate the anomalous registration result. However, if the study area is rugged or mountainous and rigorous change detection is needed, topographic correction may be necessary but cannot be addressed using the conventional polynomial transformation method. In this study, we used collinearity equation and adopted a rigorous orthorectification method which utilizes digital elevation model (DEM) and sensor position information to remove the geometric distortion inherent in imagery caused by sensor orientation, topographic relief displacement and systematic errors associated with imagery. The 2003 SPOT image was first orthorectified using a digital orthorectified map (DOM) of the same year as the reference image, and meanwhile DEM with 25 m interval and sensor information from metadata as assistant data. After that, if eligible, the 2003 orthorectified SPOT image was then accepted as the reference image for the other three images to finish the image-to-image rectification and registration simultaneously. Table 2 shows the geometric correction accuracy by using orthorectification method.

Table 2. The geometric correction accuracy using orthorectification method.

Acquisition Date	Method	Number of Ground Control Points (GCPs)	Total RMS
06-03-2003	Orthorectification	22	0.4264
06-03-2003	Polynomial Transformation	22	0.6132
25-03-2016	Orthorectification	28	0.4085
21-12-2006	Orthorectification	30	0.4275
29-03-2000	Orthorectification	26	0.4191
22-04-1996	Orthorectification	27	0.4291

As for atmospheric correction or normalization, a number of studies have demonstrated that it is unnecessary and even possible to ignore atmospheric effects when change detection is based on classification of multi-date composite imagery in which the multiple dates of remotely sensed images are rectified and placed in a single dataset and then classified as if it were a single image (e.g., multiple-date principle components detection) [41,43,44,48,49]. Meantime, operational and effective atmospheric correction methods for multi-sensor and multi-mode datasets were unavailable, up to now. On the other hand, successful change detection can be archived without atmospheric correction. It would be a real success of this study and has the potential for extended application. Furthermore, PCA has the advantage of automatically calibrating exogenous differences to the extent that these differences have an overall linear effect on the remotely sensed signal [50,51]. Therefore, bearing this consideration in mind, multi-temporal atmospheric correction or normalization was not implemented in this study. In addition, the spatial resolution of our SPOT images was 10 and 20 m, so the images were resampled to 10 m spatial resolution before change detection.

2.3.3. Multi-Date PCA for Enhancement Change Information

PCA is a multivariate statistical technique that transforms the original remotely sensed dataset into a smaller and easier dataset to interpret set of uncorrelated variables which represent most of the information in the original dataset [44,52,53]. PCA-based change detection has become one of the most popular techniques and shown better performance compared with other change detection techniques in many studies because of its simplicity and capability of enhancing the information on change [43,54–61].

In this study, multi-date merged PCA was adopted to detect changes in which the images with n/m bands taken at two different times are combined into one image with (n + m) bands, and then the combined bands are transformed into (n + m) PCs (Figure 2). Fortunately, most information

content was compressed into the first few PCs and, simultaneously, land use changes were highlighted and enhanced in according principal components. Figures 3 and 4 are examples for the land change information from cropland and water to urban land (used for housing, Figures 3c and 4c) enhanced by PCA. Figures 5 and 6 are also examples for the PCA-enhanced land change information where cropland and water were encroached for building the Economic and Technological Development Zone and new University Parks.
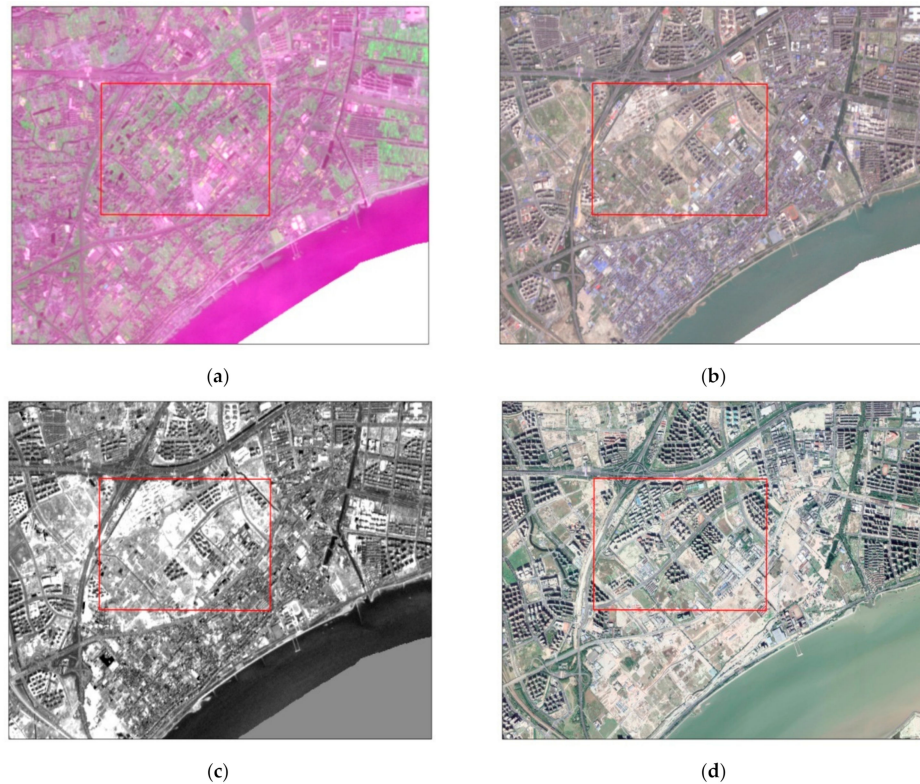

(a)

(b)

(c)

(d)

Figure 3. Example of Principal Component Analysis (PCA)-enhanced land use change information from cropland and water to urban land in the third principal component (PC3), 2006–2016. (**a**) Red, Green and Blue (RGB) composition image of SPOT-5 (2006); (**b**) RGB composition image of Sentinel-2A (2016); (**c**) the third principal component; (**d**) GF-2 image (2016).
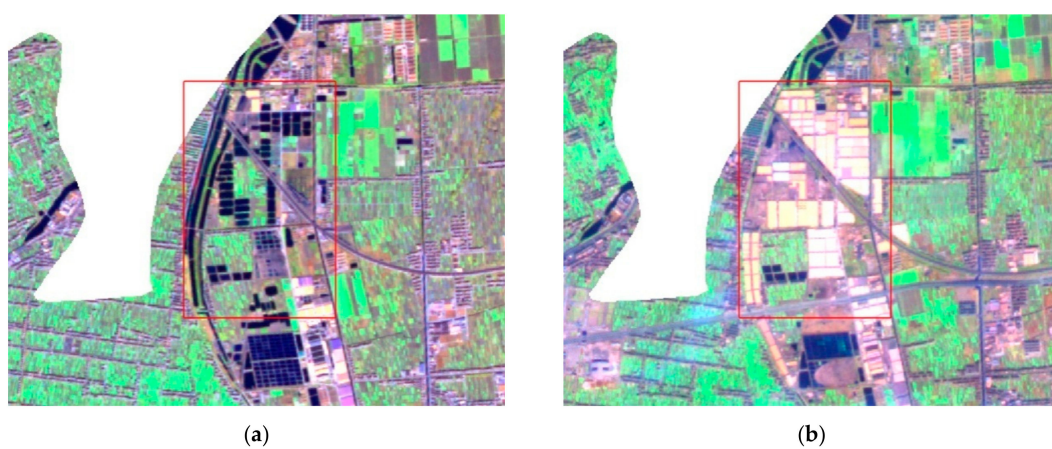

(a)

(b)

Figure 4. *Cont.*

(**c**)

(**d**)

Figure 4. Example of PCA-enhanced land use change information from cropland and water to urban land in the third principal component (PC3), 2003–2006. (**a**) RGB composition image of SPOT-5 (2003); (**b**) (RGB) composition image of SPOT-5 (2006); (**c**) the third principal component; (**d**) field survey photo (2006).

(**a**)

(**b**)

(**c**)

(**d**)

(**e**)

(**f**)

(**g**)

(**h**)
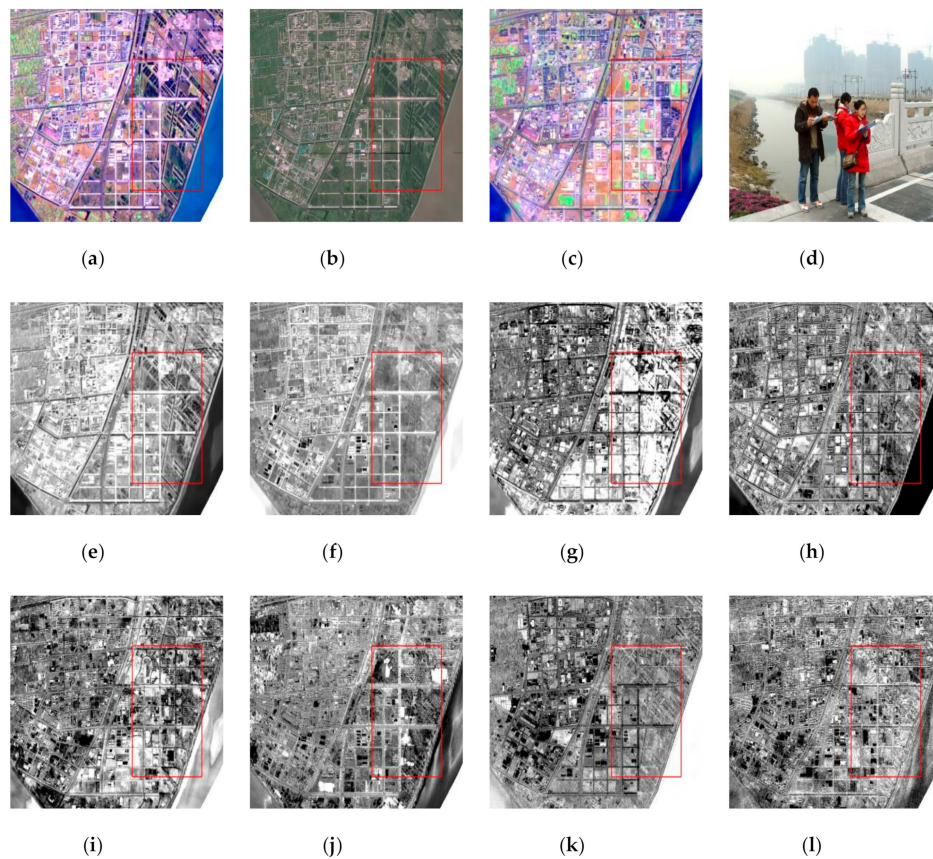

(**i**)

(**j**)

(**k**)

(**l**)

Figure 5. Example of multi-date PCA land use change enhancement, 2003–2006. (**a**) RGB composition image of SPOT-3 (2003); (**b**) color aerial photograph (2000); (**c**) RGB composition image of SPOT-5 (2006); (**d**) field survey photo (2006); (**e**–**l**) from the first to eighth principal components (PC1–PC8).
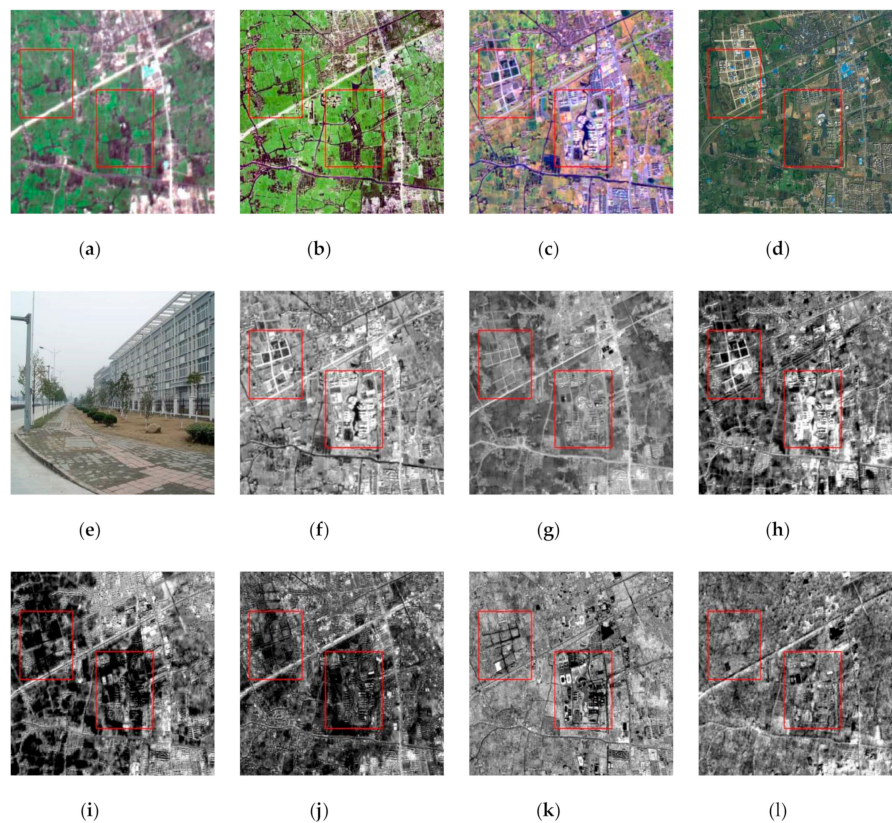
Figure 6. Example of multi-date PCA land use change enhancement, 2000–2003. (**a**) RGB composition image of SPOT-3 (2000); (**b**) color aerial photograph (2000); (**c**) RGB composition image of SPOT-5 (2003); (**d**) RGB composition image of IKONOS (2003); (**e**) field survey photo (2003); (**f–l**) from the first to seventh principal components (PC1–PC8).

2.3.4. Hybrid Classifier for Extraction Change Information

For land use change being enhanced, an essential and crucial step is to extract and then obtain "from-to" change information using classification methods. Consequently, selecting suitable and operational classification will have considerable impacts on the whole accuracy of the change detection procedure.

In this study, an operational hybrid classifier combining an unsupervised and supervised approached was adopted and conducted on the PCA-enhanced change images (Figure 2). It is an extension of a method successfully used in a tentative study, which has demonstrated the potential to provide accurate change detection information [54]. The greatest challenge to the successful application of the spectral change detection identification methods is the discrimination of "change" and "no-change" pixels from the continuous spread of data [46]. Thus, the use of Iterative Self-Organizing Data Analysis Technique (ISODATA) unsupervised classification was first performed on multi-temporal PCA-enhanced images to produce unlabeled cluster maps and, at the same time, provide a basic set of classes for further supervised classification. After empirical tries of 30, 40, 50, 60 and 80, the number of clustering classes, deemed as the most important parameter, of 60 was determined as the optimum number considering the tradeoff between precision and processing costs. Referencing on the land use map, aerial photograph, field survey data and other ancillary data, all the clusters of different changing periods were examined and assigned into three categories: obvious changed, unchanged (such as cropland, urban land) and uncertain land use (mainly referring to unidentified classes). Then, taking uncertain land use as the mask template, multi-temporal PCA-enhanced images were masked to remove the obvious changed and unchanged pixels respectively. Following, Maximum Likelihood (ML) supervised classification was implemented on masked images with the same reference

date as unsupervised for training samples. Finally, land use change maps for four periods were achieved by integrating the classification outcome that resulted from unsupervised and supervised classifiers, respectively.

2.3.5. Post-Classification Comparison Change Detection

In order to evaluate the performance and effectiveness of the proposed method as compared with the conventional method, the post-classification comparison change detection method was also implemented (Figure 2). The ML supervised classification was performed on multi-spectral images to produce individual land use maps of each year. As the 1996 SPOT-3 PAN image made it difficult to be classified using the ML method, it was substituted by the 1996 Lansate-5 TM XS image (10 January 1996) in further change detection processes. Land use change maps of each period were derived using change detection matrix and produced the "from-to" information.

2.3.6. Accuracy Assessment

Accuracy assessment is an important preoccupation and indispensable step of the land use change application. The most common quantitative method for accuracy assessment is to apply an error matrix derived from independent classification and reference data sets [62–65]. In fact, three crucial factors: sampling strategy, reference data (ground truth data) and the total number of reference pixels will intrinsically affect the accuracy assessment.

In this study, the sampling strategy integrating stratified random sampling and user-defined plots sampling, which were designed to ensure the sampling points fairly spread in each land use change class and highlight some notable and important change class (such as cropland and urban land) synchronously, was employed in accuracy assessment in order to provide the optimum balance between statistical validity and practicality. With respect to the reference data, land use survey map, high spatial-resolution satellite imagery including IKONOS, QUICKBIRD, GF-2 and WorldView images, aerial photograph and field survey information are the main sources. Once the sample strategy and reference data were determined, the exact number of samples to be taken should be decided carefully. The number of samples is a compromise between the effort to minimize the costs of field sampling and the requirement of a minimum sample size to be representative and statistically sound [66]. Congalton [62] suggested that a good rule of thumb was to collect a minimum of 50 samples for each land-cover class in the error matrix. A total of 930 reference points (800 from stratified random and 130 from user-defined plots, respectively) were selected to assess the change detection accuracy in this study.

3. Results

For this project, the main goal is to present an accurate and practical methodology to identify changes of the major land use during the rapid urbanization process from 1996 to 2016. We divided land use into five major classes according to interest. Then great efforts and special emphasis are placed on detecting the conversion from non-urban land, especially green space land, to urban land. Consequently, a total of 12 land use and changed classes are detected and identified in this study and depicted as the following: Cropland [34]; Orchard (Or); Forest (Fo); Water (Wa); Urban Land (Ur); Cropland to Urban Land (Cr-to-Ur); Orchard to Urban Land (Or-to-Ur); Water to Urban Land (Wa-to-Ur); Forest to Urban (Fo-to-Ur); Cropland to Water (Cr-to-Wa); Crop to Orchard (Cr-to-Or); Forest to Orchard (Fo-to-Or). Land use change results are demonstrated in Figures 7–10. Accuracy assessment and comparison with the post-classification method are undertaken and analyzed according to the error matrix tables and assessing indexes.
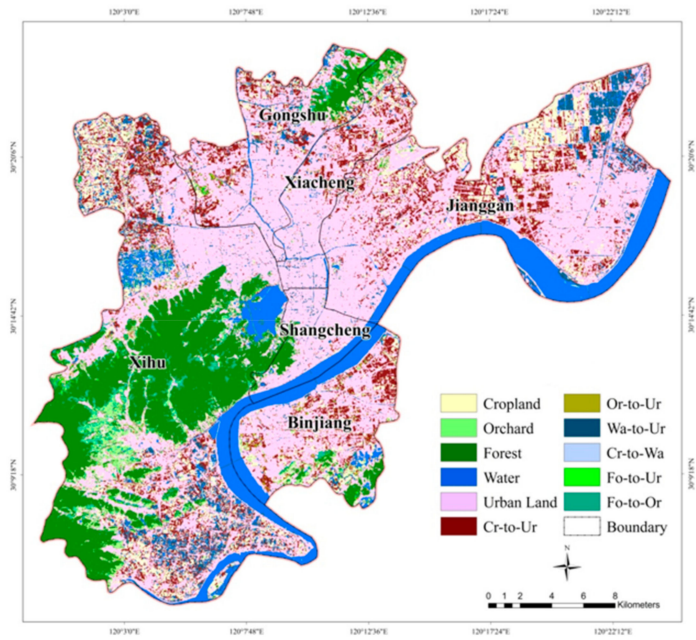
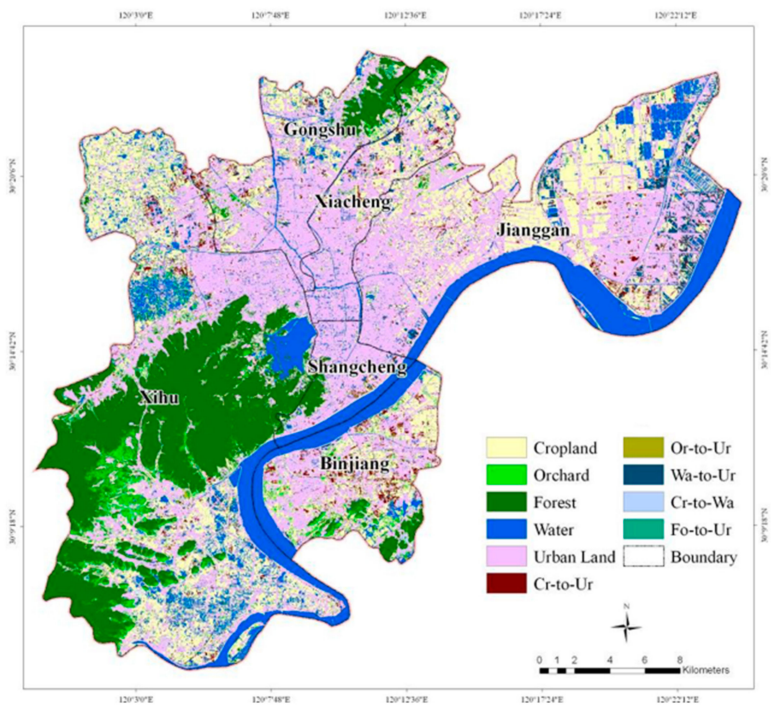**Figure 7.** Result of land use and land use changes, 2006–2016.

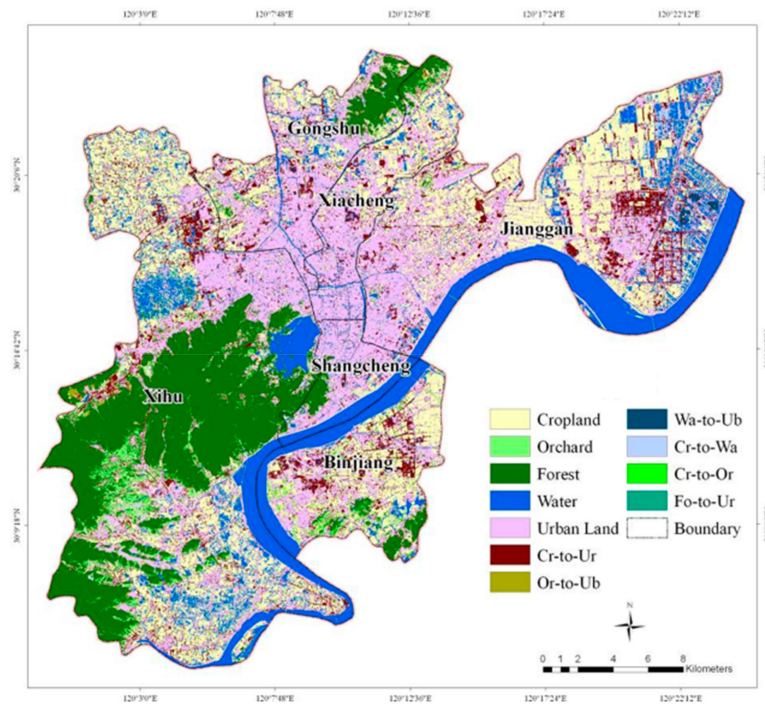

Figure 8. Result of land use and land use changes, 2003–2006.

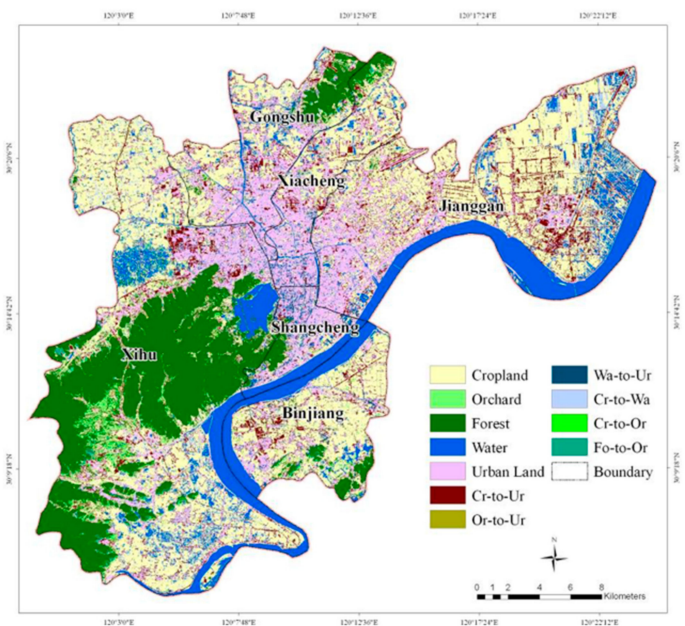**Figure 9.** Result of land use and land use changes, 2000–2003.

Figure 10. Result of land use and land use changes, 1996–2000.

3.1. Urban Expansion and Green Space Change Detection for 2006–2016

As illustrated in Figure 7, rampant urban expansion and exploitation of green space were detected during the 10-year period of 2006–2016. Concomitant with enormous land use change, a considerable high accuracy was also found according to the accuracy assessment results. The overall accuracy of change detection was calculated to be 92.90% and 0.92 for the KAPPA index (Table 3). With respect to the producer's accuracy, all classes except Cr-to-Ur exceeded 85%, with a maximum of 98.08% for Fo-to-Ur and a minimum of 89.90% for Wa, indicating that most classes were quite accurately identified. At the same time, all classes exhibited over 85% as far as the user's accuracy with a minimum of 85.48% for Wa-to-Ur. Furthermore, the comparison between error matrixes exhibits better change

detection performance of the presented PCA-based method over the post-classification method which produced the overall accuracy and KAPPA index 90.22% and 0.89 respectively (Table 3 andTable 4). However, the producer's accuracy of water and the user's accuracy of Wa-to-Ur are slightly worse than the post-classification method. The confusions are mainly caused by the misclassification and pseudo-change in classes relating to cropland and urban land.

Table 3. Confusion matrix of the PCA-based method, 2006–2016.

Classes	Reference Data											Total	Producer's Accuracy (%)	User's Accuracy (%)
	1	2	3	4	5	6	7	8	9	10	11			
1. Cr	133	1	-	1	2	7	1	-	-	-	-	145	93.66	91.72
2. Or	2	65	1	-	-	-	2	-	-	-	-	70	91.55	92.86
3. Fo	1	2	98	-	-	-	-	-	-	-	1	102	97.03	96.08
4. Wa	-	-	-	89	1	-	-	2	1	-	-	93	89.90	95.70
5. Ur	1	-	-	2	132	2	-	-	-	-	-	137	95.65	96.35
6. Cr to Ur	2	-	-	-	1	74	-	-	1	1	-	79	79.57	93.67
7. Or to Ur	-	1	-	-	-	4	52	1	-	-	-	58	92.86	89.66
8. Wa to Ur	1	-	-	5	1	2	-	53	-	-	-	62	92.98	85.48
9. Cr to Wa	2	-	-	2	1	3	-	1	60	-	-	69	96.77	86.96
10. Fo to Ur	-	1	2	-	-	1	1	-	-	51	1	57	98.08	89.47
11. Fo to Or	-	1	-	-	-	-	-	-	-	-	57	58	96.61	98.28
Total	142	71	101	99	138	93	56	57	62	52	59	930	-	-
Overall accuracy = 92.90%; Kappa coefficient = 0.92														
Cr—Cropland; Ur—Urban land Or—Orchard; Wa—Water; Fo—Forest.														

Table 4. Confusion matrix of the post-classification method, 2006–2016.

Classes	Reference Data											Total	Producer's Accuracy (%)	User's Accuracy (%)
	1	2	3	4	5	6	7	8	9	10	11			
1. Cr	130	2	2	2	1	8	1	-	-	-	-	146	91.55	89.04
2. Or	3	63	2	-	-	1	2	-	-	-	1	72	86.30	87.50
3. Fo	2	2	94	-	-	-	1	-	-	-	1	100	93.07	94.00
4. Wa	1	-	-	90	1	-	-	3	2	-	-	97	90.91	92.78
5. Ur	2	1	-	1	128	3	-	-	-	1	-	136	94.12	94.12
6. Cr to Ur	1	-	-	-	2	72	-	1	3	2	-	81	76.60	88.89
7. Or to Ur	-	1	-	-	1	3	50	1	-	-	-	56	89.29	89.29
8. Wa to Ur	1	-	-	4	1	2	-	51	-	-	-	59	89.47	86.44
9. Cr to Wa	2	-	-	2	1	3	-	1	57	-	-	66	91.94	86.36
10. Fo to Ur	-	1	2	-	1	2	1	-	-	49	1	57	94.23	85.96
11. Fo to Or	-	3	1	-	-	-	1	-	-	-	55	60	94.83	91.67
Total	142	73	101	99	136	94	56	57	62	52	58	930	-	-
Overall accuracy = 90.22%; Kappa coefficient = 0.89														

3.2. Urban Expansion and Green Space Change Detection for 2003–2006

The overall accuracy of change detection was calculated to be 92.58% and 0.92 for KAPPA index (Table 5). In terms of the producer's accuracy, all classes except Cr-to-Ur exceeded 85%, with a maximum of 100% for Fo-to-Ur and the minimum of 86.96% for Fo. It is indicated that most classes were quite accurately identified. While, Cr-to-Ur yielded the minimum producer's accuracy of 74.12% and, contrarily, the maximal omission of 25.88%. In examining the user's accuracy, most classes with the exception of Cr-to-Wa were over 80% in which the maximum of 99.02% for Fo and the minimum of 83.33% for Or-to-Ur were achieved, even now the Cr-to-Wa was close to 80% as 79.69%. Furthermore, a comparison of error matrix indicated that the proposed method generally carried out better performance than that of the post-classification in which the overall accuracy and KAPPA index were calculated to be 90.11% and 0.89, respectively (Tables 5 and 6). Similarly, with regard to the producer's and user's accuracy, most classes outperform the ones of the post-classification. However, obvious pseudo-change and misclassification were also found in the change detection result in which the main confusions tended to be pseudo Wa-to-Ur and misclassifications in Cr-to-Ur and Cr-to-Wa.

Table 5. Confusion matrix of the PCA-based method, 2003–2006.

Classes	Reference Data										Total	Producer's Accuracy (%)	User's Accuracy (%)
	1	2	3	4	5	6	7	8	9	10			
1. Cr	145	-	-	2	3	9	1	-	-	-	160	94.16	90.63
2. Or	1	67	-	-	-	-	1	-	-	-	69	93.06	97.10
3. Fo	-	1	101	-	-	-	-	-	-	-	102	98.06	99.02
4. Wa	-	-	-	100	1	1	-	1	-	-	103	86.96	97.09
5. Ur	1	-	-	1	171	2	-	-	-	-	175	95.00	97.71
6. Cr to Ur	3	-	-	-	1	63	-	-	3	-	70	74.12	90.00
7. Or to Ur	-	3	-	2	1	4	50	-	-	-	60	96.15	83.33
8. Wa to Ur	1	-	-	7	2	1	-	56	-	-	67	96.55	83.58
9. Cr to Wa	3	-	-	3	1	5	-	1	51	-	64	94.44	79.69
10. Fo to Ur	-	1	2	-	-	-	-	-	-	57	60	100.00	95.00
Total	154	72	103	115	180	85	52	58	54	57	930	-	-
Overall accuracy = 92.58%; Kappa coefficient = 0.92													

Table 6. Confusion matrix of the post-classification method, 2003–2006.

Classes	Reference Data										Total	Producer's Accuracy (%)	User's Accuracy (%)
	1	2	3	4	5	6	7	8	9	10			
1. Cr	140	1	-	2	4	10	1	-	-	-	158	90.91	88.61
2. Or	2	64	2	-	-	-	2	-	-	-	70	88.89	91.43
3. Fo	1	3	99	-	-	-	-	-	-	-	103	96.12	96.12
4. Wa	1	-	-	99	1	1	-	1	1	-	104	86.09	95.19
5. Ur	1	-	-	1	167	3	-	-	1	-	173	92.78	96.53
6. Cr to Ur	3	-	-	0	3	61	-	-	4	-	71	71.76	85.92
7. Or to Ur	-	3	-	2	1	1	48	-	-	-	55	92.31	87.27
8. Wa to Ur	1	-	-	8	2	1	-	56	-	1	69	96.55	81.16
9. Cr to Wa	5	-	-	3	2	8	-	1	48	-	67	88.89	71.64
10. Fo to Ur	-	1	2	-	-	-	1	-	-	56	60	98.25	93.33
Total	154	72	103	115	180	85	52	58	54	57	930	-	-
Overall accuracy = 90.11%; Kappa coefficient = 0.89													

3.3. Urban Expansion and Green Space Change Detection for 2000–2003

Satisfying change detection results were also found according to the accuracy assessment from Table 7. The overall accuracy was calculated to be 90.43% and 0.89 for KAPPA index. With respect to the producer's accuracy, all classes showed over 80% with a maximum of 100% for Cr-to-Or and a minimum of 80.13% for Ur. Similarly, most classes except Cr-to-Ur and Cr-to-Or exhibited over 80% as far as the user's accuracy. What is more, the comparison between error matrixes confirms the better accuracy produced by the PCA-based method over the post-classification method, which results in the overall accuracy and KAPPA indexes 90.43% and 0.89 respectively (Tables 7 and 8). At the time, most classes resulted from the PCA-based method exceed the ones of the post-classification referring to the producer's and user's accuracy. Noticeable land use change confusions were also identified during the change detection process and more serious than the case of 2003–2006. The pseudo changes from cropland, water and forest to urban land and misclassifications in classes relating to cropland, orchard and urban land dominate the confusions.

Table 7. Confusion matrix of the PCA-based method, 2000–2003.

Classes	Reference Data											Total	Producer's Accuracy (%)	User's Accuracy (%)
	1	2	3	4	5	6	7	8	9	10	11			
1. Cr	147	1	-	1	4	6	-	-	1	-	-	160	91.88	91.88
2. Or	2	63	1	-	-	-	-	-	-	-	-	66	87.50	95.45
3. Fo	-	-	90	-	1	-	-	-	-	-	-	91	90.91	98.90
4. Wa	-	1	-	92	3	-	-	-	1	-	-	97	95.83	94.85
5. Ur	1	1	-	1	121	1	-	-	-	-	-	125	80.13	96.80
6. Cr to Ur	4	-	-	-	17	60	1	2	-	-	1	85	80.00	70.59
7. Or to Ur	-	-	-	-	-	1	58	-	-	-	1	60	95.08	96.67
8. Wa to Ur	-	-	-	-	4	2	-	55	-	-	-	61	96.49	90.16
9. Cr to Wa	2	-	-	2	1	-	-	-	58	-	-	63	96.67	92.06
10. Cr to Or	4	5	-	-	-	2	-	-	-	51	-	62	100.00	82.26
11. Fo to Ur	-	1	8	-	-	3	2	-	-	-	46	160	95.83	76.67
Total	160	72	99	96	151	75	61	57	60	51	48	930	-	-
Overall accuracy = 90.43%; Kappa coefficient = 0.89														

Table 8. Confusion matrix of the post-classification method, 2000–2003.

Classes	Reference Data											Total	Producer's Accuracy (%)	User's Accuracy (%)
	1	2	3	4	5	6	7	8	9	10	11			
1. Cr	141	2	1	1	7	7	-	-	1	1		161	88.13	87.58
2. Or	3	63	2	-	-	-	1	-	-	1	-	70	87.50	90.00
3. Fo	1	1	88	-	1	-	-	-	-	-	1	92	88.89	95.65
4. Wa	2	1	-	89	3	-	-	-	2	-		97	92.71	91.75
5. Ur	1	1	-	3	117	3	-	1	-	-		126	77.48	92.86
6. Cr to Ur	5	-	-	-	18	54	2	2	1	-	1	83	72.00	65.06
7. Or to Ur	1	1	2	-	-	1	56	-	-	-	1	62	91.80	90.32
8. Wa to Ur	-	-	-	1	4	3	-	53	-	-	1	62	92.98	85.48
9. Cr to Wa	2	-	-	2	1	-	-	1	56	-	-	62	93.33	90.32
10. Cr to Or	4	2	-	-	-	4	-	-	-	49	-	59	96.08	83.05
11. Fo to Ur	-	1	6	-	-	3	2	-	-	-	44	56	91.67	78.57
Total	160	72	99	96	151	75	61	57	60	51	48	930	-	-
Overall accuracy = 87.1%; Kappa coefficient = 0.86														

3.4. Urban Expansion and Green Space Change Detection for 1996–2000

Compared with the cases of 2006–2016, 2003–2006 and 2000–2003, slightly worse accuracy was achieved but, even now, the overall accuracy and KAPPA indexes were still determined to be 88.39% and 0.87 respectively (Table 9). Most classes excluding Ur and Cr-to-Ur yielded over or close to 90% accuracy in looking into the producer's accuracy. As for the user's accuracy, each class showed over 75% with the exception of Wa-to-Ur and Cr-to-Ur. Whereas, these two classes really produced significant commission which may be the outcome of the relatively coarse resolution of multi-sensors. Consequently, considerable confusions which are the most serious among the three cases are found in the results, especially the pseudo change in Cr-to-Wa and the misclassification in Wa-to-Ur and minor confusion in cropland-related transformation. However, the comparison of error matrix exhibits that the proposed method outperforms the post-classification (Tables 9 and 10).

Table 9. Confusion matrix of the PCA-based method, 1996–2000.

Classes	Reference Data											Total	Producer's Accuracy (%)	User's Accuracy (%)
	1	2	3	4	5	6	7	8	9	10	11			
1. Cr	183	5	-	1	1	1	-	-	-	-	-	191	89.27	95.81
2. Or	-	62	2	-	-	-	1	-	-	-	-	65	89.86	95.38
3. Fo	-	-	91	-	-	-	-	-	-	-	1	92	92.86	98.91
4. Wa	1	-	-	88	1	1	-	-	-	-	-	91	95.65	96.70
5. Ur	-	-	-	-	96	3	-	-	-	-	-	99	75.00	96.97
6. Cr to Ur	-	-	-	-	7	69	1	2	1	-	-	80	74.19	86.25
7. Or to Ur	-	-	-	2	5	-	54	-	-	-	-	61	91.53	88.52
8. Wa to Ur	-	-	-	1	17	5	-	40	-	-	-	63	95.24	63.49
9. Cr to Wa	18	-	-	-	-	6	-	-	42	1	-	67	95.45	62.69
10. Cr to Or	3	-	-	-	-	8	3	-	1	45	-	60	95.74	75.00
11. Fo to Or	-	2	5	-	1	-	-	-	-	1	52	61	98.11	85.25
Total	205	69	98	92	128	93	59	42	44	47	53	930	–	–
Overall accuracy = 88.39%; Kappa coefficient = 0.87														

Table 10. Confusion matrix of the post-classification method, 1996–2000.

Classes	Reference Data											Total	Producer's Accuracy (%)	User's Accuracy (%)
	1	2	3	4	5	6	7	8	9	10	11			
1. Cr	177	2	-	1	1	1	-	-	-	-	-	182	86.34	97.25
2. Or	2	60	2	-	-	-	1	-	-	-	-	65	86.96	92.31
3. Fo	1	-	90	-	-	1	-	-	-	-	2	94	91.84	95.74
4. Wa	2	-	-	88	1	1	-	1	-	-	-	93	95.65	94.62
5. Ur	2	-	-	-	95	5	-	1	-	-	-	103	74.22	92.23
6. Cr to Ur	2	-	-	-	7	65	1	2	1	-	-	78	69.89	83.33
7. Or to Ur	-	4	-	2	5	-	54	-	-	-	-	65	91.53	83.08
8. Wa to Ur	-	-	-	1	18	6	-	38	-	-	-	63	90.48	60.32
9. Cr to Wa	15	-	-	-	-	6	-	-	42	1	-	64	95.45	65.63
10. Cr to Or	4	-	-	-	-	8	3	-	1	45	-	61	95.74	73.77
11. Fo to Or	-	3	6	-	1	-	-	-	-	1	51	62	96.23	82.26
Total	205	69	98	92	128	93	59	42	44	47	53	930	–	–
Overall accuracy = 86.56%; Kappa coefficient = 0.85														

4. Discussion

Based on the above-mentioned results, it is revealed that significant urban expansion process has taken place spanning 20 years during which dramatic transformation from non-urban land to urban land use has also been monitored. Fortunately, the land use change has been accurately identified and extracted using the presented methodology during four periods which provide a reliable foundation for monitoring. The reasonable and approving overall accuracies are accordingly yielded which exceed the minimum standard of 85% stipulated by the U.S. Geological Survey classification scheme [18]. Similarly, satisfying results are also found in most land use and changed classes with respect to the producer's accuracy and user's accuracy. Further, the comparison with the conventional post-classification method confirms the effectiveness of this methodology for monitoring urban expansion and land use change.

Precise geometric correction is substantially crucial for multi-temporal land use change detection. The orthorectification produced obviously more accurate geometric fidelity than that of polynomial method with the same GCPs. The total RMS of 2003 corrected SPOT Level 1A image was 0.4264 and 0.6132 for orthorectification and polynomial methods, respectively. In fact, the RMS errors for the other four geometrically corrected images are all less than 0.5 pixels (Table 2). As a whole, the fine geometric corrections underlay the implementation of the multi-temporal land use change detection project.

In this study, PCA of merged multi-temporal SPOT and Sentinel image pairs commonly provide enhanced information which has been captured and consequently clearly distinguishable in different principal components. In general, it is considered that the first or second component will explain and highlight no-change as they sought to account for the maximum possible variance of the multi-date, and the later or higher components will be representative of and enhance change between two merged data [43,44,58]. For the case of 2006–2016, from Figure 3, it can be seen that the first two PCs dominate and highlight the area of no-change or common variance of the two dates. Most of the land use change information, whereas, are picked up and enhanced in the third component (PC3) in which the changed objects are bright in tone (Figures 3 and 4). However, it is important to note that the significant changes of land use and resultant landscape have exerted great influences on the result of the PCA. The assumption for the general pattern is that area of change occupies only a minor proportion of the entire study area. Unfortunately, the situation is totally disparate in the cases of 2000–2003 and 1996–2000 where land use changes took place dramatically on the entire scenes (Figures 9 and 10). The differences between the multi-sensor and multi-date data also have considerable effect to the results of PCA. Consequently, the first or second principal components do not only pick up areas of no-change as in other studies. In contrast, they enhance the change from non-urban land to urban land. For example, it is indicated from Figure 5 that changes from cropland and water to urban land are mainly enhanced in the first three components and minor changes are detected in PC6. Clearly, PCA is a scene dependent technique. Thus, even though it is a useful change enhancement technique, it should be used only with a thorough understanding of the characteristics of the study in order to avoid drawing any faulty conclusions.

Although the presented methodology may be proved practical and cost-effective, some important issues have to be noted in this study. First, obvious confusions are still found in the change detection results. These may be the outcome of the complexity of urban surface, phonological variation and atmospheric change in the study spanning 20 years. The difference in the characteristics of multi-sensor with respect to the spatial-, spectral- and radiometric-resolution, and even the sensor mode should significantly contribute to the confusion. This may answer why more confusion was found in the change detection for 1999–2000. In addition, the misregistration (or misrectification) existing in multi-date data and change detection methodology also have substantial effects on the confusion as for the technical issue.

5. Conclusions

This study has presented the usefulness of multi-date and multi-sensor SPOT and Sentinel data, PCA-based change enhancement and hybrid classification method in successfully monitoring urban

sprawl and green space change of Hangzhou City for the past 20 years. The methodology developed in this study was based on an adequate understanding of sensor characteristics, data availability, landscape features, data-related limitation, and change detection techniques employed in practice.

Due to the need to remove geometric distortion and to be used with other spatial data, orthorectification based on collinearity equation was conducted. Each of the four SPOT Level 1A images and Sentinel image were quite accurately rectified with an RMS less than 0.5 pixels which guaranteed an accurate remote sensing monitoring application. A methodology combining PCA and hybrid classification was then implemented to enhance and detect land use change. The enhanced change information was commonly captured and discriminatingly characterized in different principal components. However, the land use and pattern change, and characteristic variation in multi-source data have imposed considerable effects on the PCA. The PCA-enhanced information was classified using hybrid classifier to achieve "from-to" land use change maps of four time periods. Finally, the method integrating stratified random and user-defined plots sampling strategy with 930 reference pixels was performed on the change maps to undertake accuracy assessment. Fortunately, the result confirmed the effectiveness of the proposed methodology combining PCA and hybrid classification in extracting land use change and then providing comprehensive information on the direction and nature of urban expansion. Sound, high accuracies of change detection were achieved for four changing periods referring to the overall accuracy and KAPPA indexes. The user's and producer's accuracies also show satisfying results. Furthermore, the results showed that the proposed method obviously outperformed the conventional post-classification in terms of assessment indexes. However, the efficient methods and the use of satellites with finer spatial resolution are still a promising and attractive direction and can be used for urban expansion and green space dynamics in remote sensing, all the time.

Conflicts of Interest: The authors declare no conflict of interest.

References

1.　Chen, S.S.; Chen, L.F.; Liu, Q.H.; Li, X.; Tan, Q. Remote sensing and GIS-based integrated analysis of coastal changes and their environmental impacts in Lingding Bay, Pearl River Estuary, South China. *Ocean Coast. Manag.* **2005**, *83*, 65–83. [CrossRef]

2.　Ji, C.Y.; Liu, Q.H.; Sun, D.F.; Wang, S.; Lin, P.; Li, X.W. Monitoring urban expansion with remote sensing in china. *Int. J. Remote Sens.* **2001**, *22*, 1441–1455. [CrossRef]

3.　Weng, Q. A remote sensing? Gis evaluation of urban expansion and its impact on surface temperature in the zhujiang delta, china. *Int. J. Remote Sens.* **2001**, *22*, 1999–2014. [CrossRef]

4.　Yeh, A.G.O.; Li, X. Economic development and agricultural land loss in the pearl river delta, china. *Habitat Int.* **1999**, *23*, 373–390. [CrossRef]

5.　Yeh, A.G.O.; LI, X. Measurement and monitoring of urban sprawl in a rapidly growing region using entropy. *Photogramm. Eng. Remote Sens.* **2001**, *63*, 83–90.

6.　Dahmann, N.; Wolch, J.; Joassart-Marcelli, P.; Reynolds, K.; Jerrett, M. The active city? Disparities in provision of urban public recreation resources. *Health Place* **2010**, *16*, 431–445. [CrossRef]

7.　Sister, C.; Wolch, J.; Wilson, J. Got green? Addressing environmental justice in park provision. *GeoJournal* **2010**, *75*, 229–248. [CrossRef]

8.　Wolch, J.R.; Byrne, J.; Newell, J.P. Urban green space, public health, and environmental justice: The challenge of making cities 'just green enough'. *Landsc. Urban Plan.* **2014**, *125*, 234–244. [CrossRef]

9.　Zhou, X.; Wang, Y.C. Spatial–temporal dynamics of urban green space in response to rapid urbanization and greening policies. *Landsc. Urban Plan.* **2011**, *100*, 268–277. [CrossRef]

10.　Maas, J.; Verheij, R.A.; Groenewegen, P.P.; De, V.S.; Spreeuwenberg, P. Green space, urbanity, and health: How strong is the relation? *J. Epidemiol. Community Health* **2006**, *60*, 587–592. [CrossRef] [PubMed]

11.　Wan, L.; Ye, X.; Lee, J.; Lu, X.; Zheng, L.; Wu, K. Effects of urbanization on ecosystem service values in a mineral resource-based city. *Habitat Int.* **2015**, *46*, 54–63. [CrossRef]

12.　Awotwi, A.; Anornu, G.K.; Quaye-Ballard, J.; Annor, T.; Forkuo, E.K. Analysis of climate and anthropogenic impacts on runoff in the lower pra river basin of ghana. *Heliyon* **2017**, *3*. [CrossRef]

13.　Dimitrov, S.; Georgiev, G.; Georgieva, M.; Gluschkova, M.; Chepisheva, V.; Mirchev, P.; Zhiyanski, M. Integrated assessment of urban green infrastructure condition in karlovo urban area by in-situ observations and remote sensing. *One Ecosyst.* **2018**, *3*, e21610. [CrossRef]

14.　Howison, R.A.; Piersma, T.; Kentie, R.; Hooijmeijer, J.C.; Olff, H. Quantifying landscape-level land-use intensity patterns through radar-based remote sensing. *J. Appl. Ecol.* **2018**, *55*, 1276–1287. [CrossRef]

15.　Barnsley, M.J.; Barr, S.L. Inferring urban land use from satellite sensor images using kernel-based spatial reclassification. *Photogramm. Eng. Remote Sens.* **1996**, *62*, 949–958.

16.　Colwell, R.N. Spot simulation imagery for urban monitoring: A comparison with Landsat TM and MSS imagery and with high altitude color infrared photograph. *Photogramm. Eng. Remote Sens.* **1985**, *51*, 1093–1101.

17.　Donnay, J.P.; Barnsley, M.; Longley, P. *Remote Sensing and Urban Analysis-Introduction*; Taylor & Francis: London, UK, 2001.

18.　Anderson, J.R. *A Land Use and Land Cover Classification System for Use with Remote Sensor Data*; US Government Printing Office: Boston, MA, USA, 1976; Volume 964.

19.　Lo, C.P. *Applied Remote Sensing*; Longman: New York, NY, USA, 1986.

20.　Yang, X.; Lo, C.P. Using a time series of satellite imagery to detect land use and land cover changes in the atlanta, georgia metropolitan area. *Int. J. Remote Sens.* **2002**, *23*, 1775–1798. [CrossRef]

21.　Atkinson, P.M.; Curran, P.J. Choosing an appropriate spatial resolution for remote sensing investigations. *Photogramm. Eng. Remote Sens.* **1997**, *63*, 1345–1351. [CrossRef]

22.　Curran, P.J.; Williamson, H.D. Sample-size for ground and remotely sensed data. *Remote Sens. Environ.* **1986**, *20*, 31–41. [CrossRef]

23.　Lu, D.; Mausel, P.; Brondizio, E.; Moran, E. Change detection techniques. *Int. J. Remote Sens.* **2004**, *25*, 2365–2401. [CrossRef]

24.　Qian, Y.G.; Zhou, W.Q.; Yu, W.J.; Pickett, S.T.A. Quantifying spatiotemporal pattern of urban greenspace: New insights from high resolution data. *Landsc. Ecol.* **2015**, *30*, 1165–1173. [CrossRef]

25.　Welch, R. Spatial resolution requirements for urban studies. *Int. J. Remote Sens.* **1982**, *3*, 139–146. [CrossRef]

26.　Li, X.; Zhou, W.; Huang, L.; Hao, J.; Zou, R. Rearch and application of dynamic monitoring in land use. *Econ. Geogr.* **2008**, *4*. [CrossRef]

27.　Liu, F.; Zhang, Z.; Wang, X. Forms of urban expansion of chinese municipalities and provincial capitals, 1970s–2013. *Remote Sens.* **2016**, *8*, 930. [CrossRef]

28.　Liu, W.; Liu, J.; Kuang, W.; Ning, J. Examining the influence of the implementation of Major Function-oriented Zones on built-up area expansion in China. *J. Geogr. Sci.* **2017**, *27*, 643–660. [CrossRef]

29.　Uamkasem, B.; Chao, H.L.; Jiantao, B. Regional land use dynamic monitoring using Chinese GFF high resolution satellite data. Proccedings of the 2017 International Conference on Applied System Innovation (ICASI), Sapporo, Japan, 13–17 2017.

30.　Wang, H.; Wang, C.; Wu, H. Using GF-2 imagery and the conditional random field model for urban forest cover mapping. *Remote Sens. Lett.* **2016**, *7*, 378–387. [CrossRef]

31.　Forkuor, G.; Dimobe, K.; Serme, I.; Tondoh, J.E. Landsat-8 vs. Sentinel-2: Examining the added value of sentinel-2's red-edge bands to land-use and land-cover mapping in burkina faso. *GISci. Remote Sens. Environ.* **2018**, *55*, 331–354. [CrossRef]

32.　Che, M.; Gamba, P. Intra-urban change analysis using Sentinel-1 and Nighttime Light Data. *IEEE J. Sel. Top. Appl. Earth Obs. Remote Sens.* **2019**, *12*, 1134–1143. [CrossRef]

33.　Clerici, N.; Valbuena Calderón, C.A.; Posada, J.M. Fusion of Sentinel-1a and Sentinel-2a data for land cover mapping: A case study in the lower magdalena region. *Colomb. J. Maps* **2017**, *13*, 718–726. [CrossRef]

34. Crosetto, M.; Budillon, A.; Johnsy, A.; Schirinzi, G.; Devanthéry, N.; Monserrat, O.; Cuevas-González, M. Urban monitoring based on Sentinel-1 data using permanent scatterer interferometry and sar tomography. *International archives of the photogrammetry. Remote Sens. Spat. Inf. Sci.* **2018**, *42*. [CrossRef]

35. Kopecká, M.; Szatmári, D.; Rosina, K. Analysis of urban green spaces based on Sentinel-2a: Case studies from slovakia. *Land* **2017**, *6*, 25. [CrossRef]

36. Singh, K.K. Urban green space availability in bathinda city, india. *Environ. Monit. Assess.* **2018**, *190*, 671. [CrossRef]

37. Coppin, P.R.; Bauer, M.E. Digital change detection in forest ecosystems with remote sensing imagery. *Remote Sens. Rev.* **1996**, *13*, 207–234. [CrossRef]

38. Lunetta, R.S.; Elvidge, C.D. *Remote Sensing Change Detection: Environmental Monitoring Methods and Applications*; MI Ann Arbor Press:: Chelsea, UK, 1999.

39. Nelson, R.F. Detecting forest canopy change due to insect activity using Landsat MSS. *Photogramm. Eng. Remote Sens.* **1983**, *49*, 1303–1314.

40. Pilon, P.G.; Howarth, P.J.; Bullock, R.A.; Adeniyi, P.O. An enhanced classification approach to change detection in semi-arid environments. *Photogramm. Eng. Remote Sens. Environ.* **1988**, *54*, 1709–1716.

41. Singh, A. Review article digital change detection techniques using remotely-sensed data. *Int. J Remote Sens.* **1989**, *10*, 989–1003. [CrossRef]

42. Coppin, P.; Jonckheere, I.; Nackaerts, K.; Muys, B.; Lambin, E. Digital change detection methods in ecosystem monitoring: A review. *Int. J. Remote Sens.* **2004**, *25*, 1565–1596. [CrossRef]

43. Collins, J.B.; Woodcock, C.E. An assessment of several linear change detection techniques for mapping forest mortality using multitemporal Landsat TM data. *Remote Sens. Environ.* **1996**, *56*, 66–77. [CrossRef]

44. Jensen, J.R. *Introductory Digital Image Processing: A Remote Sensing Perspective*; Prentice Hall Press: Upper Saddle River, NJ, USA,, 2015.

45. Yuan, D.; Elvidge, C.D. Nalc land cover change detection pilot study: Washigton D.C. Area experiment. *Remote Sens. Environ.* **1998**, *66*, 166–178. [CrossRef]

46. Yuan, D.; Elvidge, C.D. Survey of Multispectral Methods for Land Cover Change Analysis. In *Remote Sensing Change Detection: Environment Monitoring Methods and Applications*; Ann Arbo Press: Chelsea, UK, 1998.

47. Giangrave, D.L.; Bauer, L.A.; DeBenedictis, M.P.; Vaughan, Z.L. *Measuring Green Space Efficacy in Hangzhou, China*; Worcester Polytechnic Institute: Worcester, MA, USA, 2018.

48. Kawata, Y.; Ohtani, A.; Kusaka, T.; Ueno, S. Classification accuracy for the MOS-1 MESSR data before and after the atmospheric correction. *IEEE Trans. Geosci. Remote Sens. Environ.* **1990**, *28*, 755–760. [CrossRef]

49. Song, C.; Woodcock, C.E.; Seto, K.C.; Lenney, M.P.; Macomber, S.A. Classification and change detection using Landsat TM data: When and how to correct atmospheric effects? *Remote Sens. Environ.* **2001**, *75*, 230–244. [CrossRef]

50. Chavez, P.S.; Mackinnon, D.J. Automatic detection of vegetation changes in the Southwestern United-States Ssing Remotely-Sensed Images. *Photogramm. Eng. Remote Sens.* **1994**, *60*, 571–583.

51. Collins, J.B.; Woodcock, C.E. Change Detection Using the Gramm-Schmidt Transformation Applied to Mapping Forest Mortality. *Remote Sens. Environ.* **1994**, *50*, 267–279. [CrossRef]

52. Jolliffe, I.T.; Cadima, J. Principal component analysis: A review and recent developments. *Philos. Trans. R. Soc. A: Math. Phys. Eng. Sci.* **2016**, *374*, 20150202. [CrossRef]

53. Schowengerdt, R.A. *Remote sensing: Models and Methods for Image Processing*; Academic Press: Valencia, CA, USA, 1997.

54. Deng, J.S.; Wang, K.; Li, J.; Shen, Z.Q. PCA-based land-use change detection and analysis using multitemporal and multisensor satellite data. *Int. J. Remote Sens.* **2008**, *29*, 4823–4838. [CrossRef]

55. Eastman, J.R.; Fulk, M. Long sequence time series evaluation using standardized principal components. *Photogramm. Eng. Remote Sens.* **1993**, *59*, 991–996.

56. Fung, T.; LeDrew, E. Application of principal components analysis to change detection. *Photogramm. Eng. Remote Sens. Environ.* **1987**, *53*, 1649–1658.

57. Ingebritsen, S.E.; Lyon, R.J.P. Principal components analysis of multitemporal image pairs. *Int. J. Remote Sens.* **1985**, *6*, 687–696. [CrossRef]

58. Li, X.; Yeh, A.G.O. Principal component analysis of stacked multi-temporal images for the monitoring of rapid urban expansion in the pearl river delta. *Int J Remote Sens.* **1998**, *19*, 1501–1518. [CrossRef]

59. Lu, D.S.; Mausel, P.; Batistella, M.; Moran, E. Land-cover binary change detection methods for use in the moist tropical region of the amazon: A comparative study. *Int. J. of Remote Sens.* **2005**, *26*, 101–114. [CrossRef]

60. Mas, J.F. Monitoring land-cover changes: A comparison of change detection techniques. *Int. J. Remote Sens.* **1999**, *20*, 139–152. [CrossRef]

61. Singh, A.; Harrison, A. Standardized principal components. *Int. J Remote Sens.* **1985**, *6*, 883–896. [CrossRef]

62. Congalton, R.G. A review of assessing the accuracy of classifications of remotely sensed data. *Remote Sens. Environ.* **1991**, *37*, 35–46. [CrossRef]

63. Congalton, R.G.; Green, K. Symposium on Geoscience & Remote Sensing Symposium. In *Assessing the Accuracy of Remotely Sensed Data: Principles and Practices*; CRC Press: Boca Raton, FL, USA, 1998.

64. Foody, G.M. Status of land cover classification accuracy assessment. *Remote Sens. Environ.* **2002**, *80*, 185–201. [CrossRef]

65. Stehman, S.V. Practical implications of design-based sampling inference for thematic map accuracy assessment. *Remote Sens. Environ.* **2000**, *72*, 35–45. [CrossRef]

66. Dicks, S.E.; Lo, T.H.C. *Evaluation of Thematic Map Accuracy in a Land-Use and Land-Cover Mapping Program. Photogrammetric Engineering Remote Sensing of Environment*; FAO: Rome, Italy, 1990.